

# Plastic Transition to Switch Nonlinear Optical Properties Showing the Record High Contrast in a Single-Component Molecular Crystal

Zhihua Sun, Tianliang Chen, Xitao Liu, Maochun Hong, and Junhua Luo\*

Key Laboratory of Optoelectronic Materials Chemistry and Physics, Fujian Institute of Research on the Structure of Matter, Chinese Academy of Sciences, Fuzhou, Fujian 350002, P. R. China

**S** Supporting Information

**ABSTRACT:** To switch bulk nonlinear optical (NLO) effects represents an exciting new branch of NLO material science, whereas it remains a great challenge to achieve high contrast for “on/off” of quadratic NLO effects in crystalline materials. Here, we report the supereminent NLO-switching behaviors of a single-component plastic crystal, 2-(hydroxymethyl)-2-nitro-1,3-propanediol (**1**), which shows a record high contrast of at least  $\sim 150$ , exceeding all the known crystalline switches. Such a breakthrough is clearly elucidated from the slowing down of highly isotropic molecular motions during plastic-to-rigid transition. The deep understanding of its intrinsic plasticity and superior NLO property allows the construction of a feasible switching mechanism. As a unique class of substances with short-range disorder embedded in long-range ordered crystalline lattice, plastic crystals enable response to external stimuli and fulfill specific photoelectric functions, which open a newly conceptual avenue for the designing of new functional materials.

Stimuli-responsive materials are able to change their optoelectronic properties under external stimuli, such as heat, laser radiation, pressure, electric and magnetic fields, etc.<sup>1</sup> Nonlinear optical (NLO) switches, of which second-order NLO effects are reversibly converted between different states, have practical application in the emerging field of photoelectric devices.<sup>2,3</sup> Although great progress has been made for a few photochromic molecules and metal–organic complexes in liquid phase,<sup>4–7</sup> the solid-state crystalline NLO switches are still scarce. One of the great challenges is to control the alignment of noncentrosymmetric NLO moieties of new switching systems in a rational manner. A previously used strategy is to optimize conformation of “push–pull” molecules in thermochromic or photochromic compounds,<sup>8–10</sup> such as in ruthenium complexes and anil crystals. Whereas, they only display a certain reversible degree, with a limited “on/off” contrast (often 1.3–10) of tunable second harmonic generation (i.e., SHG) signals.<sup>11</sup> To develop high-contrast NLO switches, a newly conceptual scheme was recently employed, relying on structural changes. Remarkably, transformation from a centrosymmetric state to non-centrosymmetric order inspires a sharp change of NLO response and displays a feasible contrast. Mercier et al. first reported the organic–inorganic hybrids that allow the “on/off” switching of SHG effects.<sup>12</sup> This principle was further extended to other

metal–organic hybrids and multicomponent ionic salts,<sup>13–16</sup> with moderate contrast to  $\sim 35$ ; however, their gentle structural changes still restrict the “on/off” contrast. Here, we report single-component plastic crystals as a new class of solid-state NLO switches, exhibiting a record high contrast of  $\sim 150$ .

Plastic crystals are a unique class of substances, showing a co-existence of the long-range crystalline order but short-range orientational disorder.<sup>17–19</sup> Under external field, plastic state can be reversibly converted to the ordered crystalline phase, which are closely associated with the rotational and/or orientational motions. Such a conversion is highly favorable for the rational designing of NLO switches, if a well-delicate balance is created between responsive-disorder (i.e., SHG-Off) and frozen-order (SHG-On). On the other hand, a hint is that the realization of switchable NLO activities will be feasible based on plastic transitions. Despite plasticity has been known since 1960s, to the best of our knowledge, no studies of the stimuli-responsive NLO properties have been reported, and deep understanding of relationship between NLO-switching and plastic behaviors is in infancy. Here, we first investigated the switchable NLO properties of a single-component plastic molecular crystal, 2-(hydroxymethyl)-2-nitro-1,3-propanediol (**1**),<sup>20</sup> which displays a record high “on/off” contrast of  $\sim 150$ , exceeding all the known switching systems. As far as we are aware, such a promising contrast is unprecedented, although intensive research has focused on plastic materials. Besides, ordering of its highly isotropic molecular motions is closely elucidated with switchable NLO effects and unique plasticity. As an aggregative outcome of liquid and solid properties, the utilization of plasticity to switch NLO effect opens up a new strategy for the designing of stimuli-responsive materials.<sup>21</sup>

Crystals of **1** were obtained from aqueous solutions by the slow evaporation (Figure S1). Temperature-dependent NLO effects were first studied using Kurtz and Perry method, and SHG digital signals converted from photoeffects are shown in Figure 1. At room-temperature phase (RTP), **1** shows quite strong SHG activities with the intensity of  $\sim 2.5$  times larger than that of potassium dihydrogen phosphate (KDP); thus, its quadratic coefficient  $\chi^{(2)}$  is estimated as 1.37 pm/V ( $\chi^{(2)}_{\text{KDP}} \approx 0.39$  pm/V). This value is much larger than other NLO switches, such as photochromic crystals<sup>22</sup> and metal–organic frameworks,<sup>11</sup> but coincides with its polar crystal structure (Table S1). In situ measurement of NLO effects upon heating, its SHG signals were maintained over a wide temperature range until 347 K (phase

Received: October 28, 2015

Published: November 30, 2015

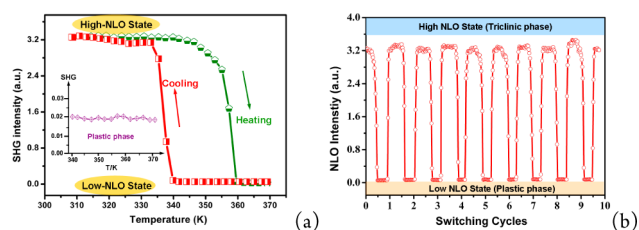


**Figure 1.** Switching of bulk NLO properties of **1**. (a) Switchable conversion of SHG signals between high-NLO and low-NLO states. (b) Completely reversible and recoverable switching of NLO effects.

transition point,  $T_c$ ),<sup>23</sup> while higher temperature leads to a complete obliteration of SHG effects. In its NLO-inactive state, no SHG signal was detected, except for quite weak noise errors (inset in Figure 1a). Hence, the NLO switching contrast of **1**, defined as the ratio of SHG intensities at high-NLO and low-NLO states, was found to be at least  $\sim 150$ .<sup>11,24</sup> Such a record high value is much higher than those for other solid-state materials reported to date ( $\sim 38$  for the metal–organic hybrids;<sup>11</sup>  $\sim 20$  for ferroelectric liquid-crystalline polymers;<sup>25</sup>  $\sim 35$  for organic ionic salts,<sup>13</sup> etc.), revealing that **1** is a fascinating candidate as NLO-switching material and makes a breakthrough in this aspect.

Another critical attribute of solid-state NLO crystalline switches is the reversible capacity, since switching-induced irreversible alignment of initial molecules severely limits the “on/off” cycles.<sup>26</sup> Here, NLO switching cycles were also performed to validate the reversibility of **1**. The key results in Figure 1b reveals that its SHG activities at high-NLO state can be recovered after several cycles without any attenuation, which discloses superior stabilities of **1** to other switching systems, including photochromic and Langmuir–Blodgett films.<sup>27</sup> All the figures of merits for **1**, including record high contrast of  $\sim 150$ , large  $\chi^{(2)}$  value of 1.37 pm/V and superior reversibility, make it exhibit higher sensitivity and lower dissipation for the potential device application in a wide transmission range (see Figure S4).

Single-crystal structure refinements of **1** were revisited at variable temperatures (Table S1). At room temperature, **1** belongs to triclinic crystallographic system with a polar space group of  $P1$ , and cell parameters are consistent with the reported data. Its unit cell consists of two completely ordered molecules, in which three hydroxymethyl groups occupy the third-order local axes directed along C–N bond. Well-defined and perfect tetrahedrons are constructed, as revealed from the parameters of bond angles and lengths (Table S2). The  $\pi_z$ -populated orbital of nitro group interacts with one vacant orbital  $-\sigma^*(C-O)$  of the polar C–O bonds, and thus the  $\pi_z-\sigma^*$  orbital interactions can donate electron density into the orbital of  $C^{+\delta}-O^{-\delta}$  bonds.<sup>23</sup> It is interesting that oxygen atoms of carboxymethyl groups locate at the circular coping of a globule-like diagram, while the oxygen atoms of nitro groups deviate from the spheres (Figure 2a,b). Slightly distorted globular structures are thus formed with carboxymethyl groups occupying at the curvature positions of spherical architecture, which is indispensable for plastic transition. Another striking feature is that oxygen atoms of nitro groups show larger thermal ellipsoids than others, and the direction of thermal vibration ellipsoids is perpendicular to  $NO_2$  group plane (Figure 2c). In this context, nitro groups may easily overcome the energy barrier through a twisting motion, being reminiscent of the inherent short-range rotational disorder. Particularly, energy barrier will be drastically reduced for initiating a dislocation motion by weakening intermolecular

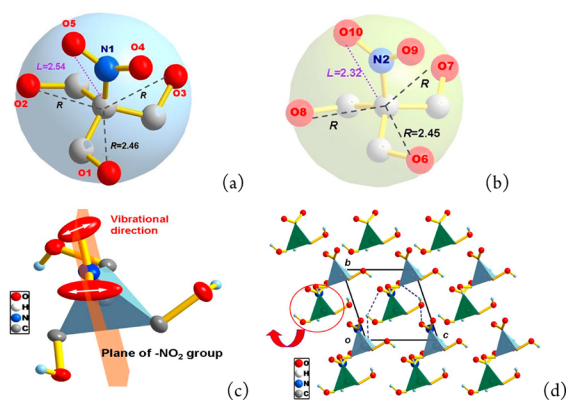


**Figure 2.** Molecular structures for **1**. (a,b) Globular-like shape of two independent molecules; (c) thermal vibrational ellipsoids for the nitro groups; and (d) crystal packing projected along the  $a$ -axis.

and/or intramolecular O–H $\cdots$ O H-bonding interactions. Figure 2d shows a polar network is formed through intermolecular O–H $\cdots$ O hydrogen bonds, and binary molecular layers arrange alternately along  $b$ -axis. Using hydrogen bonds between oxygen atoms of nearest-neighboring molecules, its packing resembles a pseudo body-centered cube (bcc) structure,<sup>28</sup> which favors the decline of potential energy barriers for the switching of NLO effects during the plastic transition.

Temperature-dependent dielectric constants and specific heat deduced from DSC confirm its crystal-to-plastic transition (Figure 3). The entropy change of  $\sim 25$  J $\cdot$ K $^{-1}$  $\cdot$ mol $^{-1}$  is larger

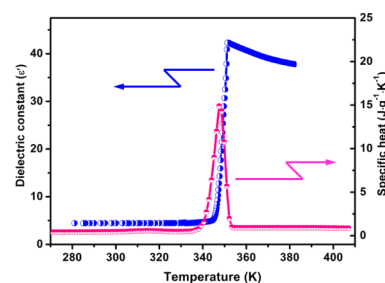


**Figure 3.** Dielectric constants and specific heat of **1**. Results of sharp anomalies reveal its crystal-to-plastic transition at 347 K.

than that of a common fusion, revealing its plastic characteristic. Variable-temperature powder X-ray patterns further disclose a pseudo bcc structure (Figure S5), being well consistent with its cell parameter of  $a = 6.898$  Å at 353 K.<sup>23</sup> This symmetry breaking resembles those in some ferroelectrics,<sup>29–31</sup> being verified by the change of NLO effects. Besides, as another indicator for plastic materials, proton conductivity of **1** shows a nonlinear sharp rise at  $T_c$ , changing from  $8.6 \times 10^{-5}$  to  $3.7 \times 10^{-4}$  S/m (Figure S6). The value of  $22.5 \times 10^{-4}$  S/m (at 380 K) is slightly smaller than that of ionic plastic materials, such as  $[Zn(HPO_4)(H_2PO_4)_2] \cdot (ImH_2)_2$  ( $\sim 2.0 \times 10^{-2}$  S/m),<sup>32</sup> but falls around those of other molecular plastic conductors (at a magnitude order of  $10^{-3}$  S/m). Such an order of magnitude increase of proton conductivity at  $T_c$  strongly confirms the plastic feature of **1**.

Solid-state NMR analysis was performed to study the nature of switchable NLO effects and molecular dynamic motions in **1**. Figure 4 shows variable-temperature NMR spectra, in which the line width at half-maximum of the peaks (denoted as line width) is used to characterize the extent of molecular motions. Below  $T_c$  (295–340 K), the intensities of  $^{13}C$  signals are almost

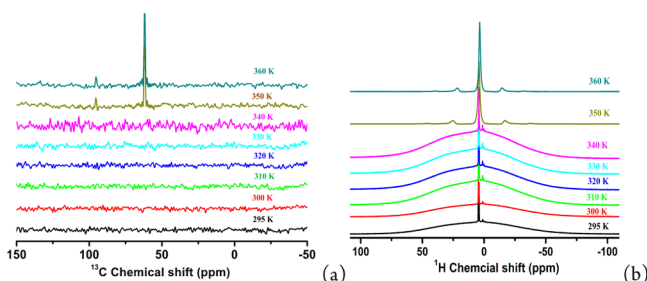


**Figure 4.** Variable-temperature NMR spectra of **1**. (a)  $^{13}\text{C}$  and (b)  $^1\text{H}$  NMR spectra. Dramatic variation of line width and area fractions of the narrow peaks are directly associated with molecular motions in plastic state.

undetectable, with the same amplitude as that of noise level. Such a low sensitivity of  $^{13}\text{C}$  NMR signals indicates that its molecular motions are largely restricted into a rigid form; namely, an orientationally ordered state. Another possibility is that the long longitudinal relaxation time of protons has a drastic effect on the sensitivity of  $^{13}\text{C}$  NMR signals. Here, a recycle delay of 2 s is sufficient to acquire  $^{13}\text{C}$  NMR signals, and thus effects of proton relaxation are reasonably ruled out. This means that the skeleton of **1** is static below  $T_c$ . Above  $T_c$ , the  $^{13}\text{C}$  spectra consist of two relatively sharp peaks. The line width of more intense low-field peak ( $\sim 59.5$  ppm, ascribed to the  $-\text{CH}_2$  group) was  $10 \pm 0.5$  ppm, while that of the high-field resonance ( $\sim 93.0$  ppm, ascribed to the central carbon) was  $8 \pm 0.5$  ppm. Such sharp peaks are indicative of the rapid overall molecular reorientations in **1**.<sup>33</sup> At even higher temperature (360 K), the line widths for  $-\text{CH}_2$  group show a slight decrease to  $\sim 8$  ppm, revealing that  $-\text{CH}_2$  groups undergo dynamic motions within a flexible architecture at plastic state.

The congenetic  $^1\text{H}$  CP/MAS NMR results also support the above-mentioned motions (Figure 4b). Below  $T_c$  (295–340 K), two distinguished parts are observed: the broad unresolved basebands and asymmetric sharp peaks ( $\sim 2.0$  and 4.1 ppm, ascribed to  $-\text{OH}$  and  $-\text{CH}_2$  groups, Figure S9) on the top of initial broad bands. The latter indicates that the structure of **1** is not fully rigid and that some motions of protons are present below  $T_c$ . Upon heating to 350 K (above  $T_c$ ), the sharp peaks combine together as a dominant peak centered at 4.5 ppm, while the broader part completely disappears. This suggests that a vast majority of the molecules undergo a translational motion. Interestingly, the highly symmetric shape of the peaks may be indicative of an isotropic globular structure, consistent with X-ray diffraction structural analyses. Besides, the narrowing of  $^1\text{H}$  line width (from 31 ppm at 350 K to 22 ppm at 360 K) suggests that the isotropic reorientation of  $\text{CH}_2$  groups increases with higher temperature, due to its low-energy barriers (about  $\sim 3.7$  kJ/mol in glass polymers).<sup>34</sup> Hence, it is proposed that those motions are likely to occur, as revealed by the  $^{13}\text{C}$  NMR spectra.

Density functional theory calculations were used to evaluate potential energies of the motions for  $\text{CH}_2\text{OH}$  and  $\text{NO}_2$  groups. Figure 5a shows that initial atomic coordinates of room-temperature structure correspond to the first potential energy minimum at  $\varphi = 0^\circ$ , of which relative potential energy ( $\Delta E$ ) was defined as zero. Meanwhile, another minimum potential is obtained at  $\varphi = 180^\circ$ , suggesting a probability of the  $180^\circ$  molecular hopping for  $\text{NO}_2$  groups at RTP. It is noteworthy that the symmetric curves exhibit two-maximum potential energy barriers at  $\varphi = 90^\circ$  and  $270^\circ$ , with  $\Delta E$  of about 54 and 51 kJ/mol, respectively. These values are reminiscent of thermal-active

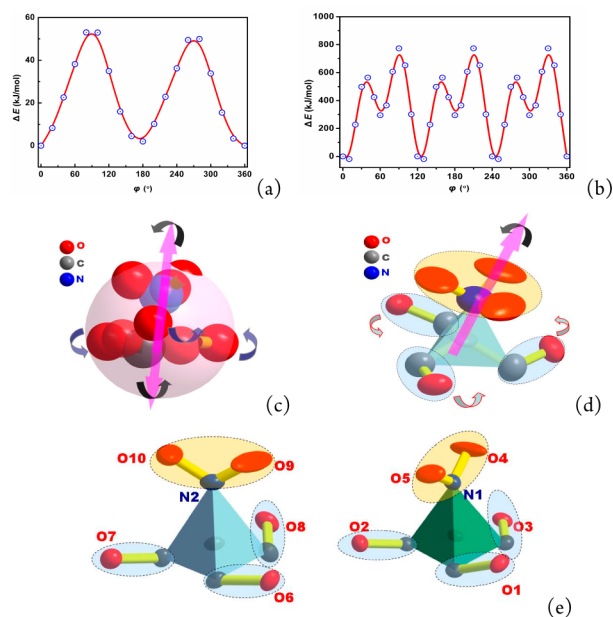


**Figure 5.** Schematic of molecular motions for **1** at different states. (a,b) Diagrams of the simulated potential energy barriers for the rotations of  $-\text{NO}_2$  and  $-\text{CH}_2\text{OH}$  groups, respectively. (c) Whole molecular rotation and reorientation at plastic phase; (d) rotational mode along central C–N axis at 345 K; and (e) rigid-state below  $T_c$ . The skeleton is almost frozen except for dynamic motions of protons (from  $^1\text{H}$  NMR spectra).

behaviors of nitro groups, due to the relatively low activation energy barrier ( $\sim 3.8$  kcal/mol).<sup>35</sup> Although nitro groups are initially ordered below  $T_c$ , their easily activated deformation will facilitate the fast dynamic motions in the vicinity of  $T_c$ , as revealed by large thermal ellipsoids of oxygen atoms.

Another possible motion is the rotation of  $\text{CH}_2\text{OH}$  groups. Here, the relative energy for the rotation with every  $10^\circ$  was estimated to certify the possibility of this motion (Figure 5b). A profile of rotational potentials for the three-fold symmetric sites was observed with three low-energy minima at  $\varphi = 0^\circ$ ,  $120^\circ$ , and  $240^\circ$ , respectively. However, its potential energy barriers are larger than thermal energy  $k_B T \approx 2.5$  kJ/mol (297 K),<sup>36</sup> revealing this rotational motion is almost impossible far below  $T_c$ . In contrast, structural analyses displays that an ideal  $D_{3h}$  symmetry is created for the independent molecules of **1** at 345 K, in which it adopts a positional disordered conformation (Figures S7–S8). This means that the large change of enthalpy may break its energy barriers and facilitate the occurrence of rotational motions, which agrees fairly with the situ variable-temperature  $^{13}\text{C}$  NMR spectra.

The relationship between NLO switching and plasticity is summarized as follows. In the plastic phase, **1** behaves as an active rotator with the rapid overall molecular reorientations (Figure 5c). The motions of rotation and reorientation are supposed to be the predominant mechanism, acting as the source of power for its plasticity. This manner is strongly involved with dramatic change of NMR line widths and high proton conductivity ( $22.5 \times 10^{-4}$  S/m). The optically isotropic bcc mode corresponds to its SHG-off state, in which NLO effects are fully annihilated. Approaching  $T_c$ , energy barrier for reorientation of global molecules becomes large enough to preclude thermal tumbling around their equilibrium positions. As a result, its reorientation is prohibited, and the molecules are restricted into a relatively rigid lattice. Only fast molecular motions of  $120^\circ$  rotation exists

(Figure Sd), which agrees with the population of preferentially occupied sites within the space group of R3 (crystal structure at 345 K). Such a motional-to-rigid transition is solidly supported by the dramatic decrease of proton conductivity (from  $22.5 \times 10^{-4}$  to  $8.6 \times 10^{-5}$  S/m), significant variation of NMR line widths, sharp dielectric anomalies, and large enthalpy change of specific heat. Far below  $T_c$ , all the atoms are frozen into an ordered state (SHG-on state, Figure Se), showing large NLO effects with the molecular hyperpolarizability ( $\beta_{\text{total}}$ ) and dipole moment ( $\mu_g$ ) being calculated to be  $7.74 \times 10^{-31}$  esu and  $5.72 \times 10^{-30}$  C·m, respectively (Table S4 and Figure S10).

In summary, we have demonstrated a single-component molecular plastic crystal, which exhibits switchable NLO properties with an unprecedented high-contrast up to  $\sim 150$ . This record high value exceeds all the known NLO switches and makes a breakthrough in this respect. Such a promising behavior results from the gradual slowing down of its highly isotropic molecular motions. Deep understanding of NLO-switching behavior and plasticity is clearly elucidated by combining analytical and computational methods. It is believed that the results open up a potential strategy for the designing of new stimuli-responsive materials.

## ■ ASSOCIATED CONTENT

### Supporting Information

The Supporting Information is available free of charge on the ACS Publications website at DOI: 10.1021/jacs.5b11088.

Experimental methods and data (PDF)

Crystal structure data (CIF)

## ■ AUTHOR INFORMATION

### Corresponding Author

\*jhluo@fjirsm.ac.cn

### Notes

The authors declare no competing financial interest.

## ■ ACKNOWLEDGMENTS

This work was supported by NSFC (21525104, 91422301, 21222102, 21373220, 51402296, 21171166, 21301172, 21571178, 51502290, and 51502288), and the NSF for Distinguished Young Scholars of Fujian Province (2014J06015), the NSF of Fujian Province (2014J01067, 2014J05068, and 2015J05040), and the Youth Innovation Promotion of CAS (2014262, 2015240, and 2016274). Z.S. thanks support from “Chunmiao Project” of Haixi Institute of Chinese Academy of Sciences (CMZX-2013-002). Thanks Prof. Feng Deng and Shenhui Li at Wuhan Institute of Physics and Mathematics, CAS for great help on the VT-NMR measurements.

## ■ REFERENCES

- (1) *Handbook of Stimuli-Responsive Materials*; Urban, M.W., Ed.; Wiley-VCH: Weinheim, 2011.
- (2) Delaire, J. A.; Nakatani, K. *Chem. Rev.* **2000**, *100*, 1817.
- (3) Irie, M.; Fukaminato, T.; Matsuda, K.; Kobatake, S. *Chem. Rev.* **2014**, *114*, 12174.
- (4) (a) Aubert, V.; Guerchais, V.; Ishow, E.; Hoang-Thi, K.; Ledoux, I.; Nakatani, K.; Bozec, H. L. *Angew. Chem., Int. Ed.* **2008**, *47*, 577.
- (5) Roberts, M. N.; Carling, C.-J.; Nagle, J. K.; Branda, N. R.; Wolf, M. O. *J. Am. Chem. Soc.* **2009**, *131*, 16644.
- (6) Chan, J. C.-H.; Lam, W. H.; Wong, H.-L.; Zhu, N.; Wong, W.-T.; Yam, V. W.-W. *J. Am. Chem. Soc.* **2011**, *133*, 12690.

- (7) Priimagi, A.; Ogawa, K.; Virkki, M.; Mamiya, J.-i.; Kauranen, M.; Shishido, A. *Adv. Mater.* **2012**, *24*, 6410.
- (8) Dalton, L. R.; Harper, A. W.; Robinson, B. H. *Proc. Natl. Acad. Sci. U. S. A.* **1997**, *94*, 4842.
- (9) Sullivan, P. A.; Dalton, L. R. *Acc. Chem. Res.* **2010**, *43*, 10.
- (10) Dalton, L. R.; Sullivan, P. A.; Bale, D. H. *Chem. Rev.* **2010**, *110*, 25.
- (11) Serra-Crespo, P.; Veen, M. A.; Gobechiya, E.; Houthoofd, K.; Filinchuk, Y.; Kirschhock, C. E.; Martens, J. A.; Sels, B. F.; Vos, D. E.; Kapteijn, F.; Gascon, J. *J. Am. Chem. Soc.* **2012**, *134*, 8314.
- (12) Bi, W.; Louvain, N.; Mercier, N.; Luc, J.; Rau, I.; Kajzar, F.; Sahraoui, B. *Adv. Mater.* **2008**, *20*, 1013.
- (13) Sun, Z.; Luo, J.; Zhang, S.; Ji, C.; Zhou, L.; Li, S.; Deng, F.; Hong, M. *Adv. Mater.* **2013**, *25*, 4159.
- (14) Sun, Z.; Li, S.; Zhang, S.; Deng, F.; Hong, M.; Luo, J. *Adv. Opt. Mater.* **2014**, *2*, 1199.
- (15) Sun, Z.; Chen, T.; Luo, J.; Hong, M. *Angew. Chem., Int. Ed.* **2012**, *51*, 3871.
- (16) Sun, Z.; Chen, T.; Ji, C.; Zhang, S.; Zhao, S.; Hong, M.; Luo, J. *Chem. Mater.* **2015**, *27*, 4493.
- (17) Howlett, P. C.; Shekibi, Y.; MacFarlane, D. R.; Forsyth, M. *Adv. Eng. Mater.* **2009**, *11*, 1044.
- (18) Wang, P.; Dai, Q.; Zakeeruddin, S. M.; Forsyth, M.; MacFarlane, D. R.; Grätzel, M. *J. Am. Chem. Soc.* **2004**, *126*, 13590.
- (19) Jin, L.; Nairn, K. M.; Forsyth, C. M.; Seeber, A. J.; MacFarlane, D. R. *J. Am. Chem. Soc.* **2012**, *134*, 9688.
- (20) Doshi, N.; Furman, M.; Rudman, R. *Acta Crystallogr., Sect. B: Struct. Crystallogr. Cryst. Chem.* **1973**, *29*, 143.
- (21) Liu, B.; Besseling, T. H.; Hermes, M.; Demirörs, A. F.; Imhof, A.; Blaaderen, A. *Nat. Commun.* **2014**, *5*, 3092.
- (22) Guerchais, V.; Le Bozec, H. *Topics in Organometallic Chemistry*; Springer: New York, 2010; Vol. 28, pp 171–225.
- (23) Golovina, N. I.; Raevskii, A. V.; Fedorov, B. S.; Chukanov, N. V.; Shilov, G. V.; Leonova, L. S.; Tarasov, V. P.; Erofeev, L. N. *J. Solid State Chem.* **2002**, *164*, 301.
- (24) NLO contrast was determined as the ratio of the SHG signals of RTP (high-NLO) and plastic phase (low-NLO). In its low-NLO state, the standard deviation of noise level was used as the reference.
- (25) Priimagi, A.; Ogawa, K.; Virkki, M.; Mamiya, J.-i.; Kauranen, M.; Shishido, A. *Adv. Mater.* **2012**, *24*, 6410.
- (26) Boixel, J.; Guerchais, V.; Bozec, H. L.; Jacquemin, D.; Amar, A.; Boucekkin, A.; Colombo, A.; Dragonetti, C.; Marinotto, D.; Roberto, D.; Righetto, S.; Angelis, R. D. *J. Am. Chem. Soc.* **2014**, *136*, 5367.
- (27) Atassi, Y.; Delaire, J. A.; Nakatani, K. *J. Phys. Chem.* **1995**, *99*, 16320.
- (28) Pringle, J. M.; Howlett, P. C.; MacFarlane, D. R.; Forsyth, M. *J. Mater. Chem.* **2010**, *20*, 2056.
- (29) Cai, H.-L.; Zhang, W.; Ge, J.-Z.; Zhang, Y.; Awaga, K.; Nakamura, T.; Xiong, R.-G. *Phys. Rev. Lett.* **2011**, *107*, 147601.
- (30) Fu, D.-W.; Cai, H.-L.; Liu, Y.; Ye, Q.; Zhang, W.; Zhang, Y.; Chen, X.-Y.; Giovannetti, G.; Capone, M.; Li, J.; Xiong, R.-G. *Science* **2013**, *339*, 425.
- (31) Tayi, A. S.; Kaeser, A.; Matsumoto, M.; Aida, T.; Stupp, S. I. *Nat. Chem.* **2015**, *7*, 281.
- (32) Horike, S.; Umeyama, D.; Inukai, M.; Itakura, T.; Kitagawa, S. *J. Am. Chem. Soc.* **2012**, *134*, 7612.
- (33) Andrew, E. R. *Nuclear Magnetic Resonance*; Royal Society of Chemistry: Cambridge, 1974.
- (34) Mukhopadhyay, R. In *Solid State Physics: Proceedings of the D.A.E. Solid State Physics Symposium*; Mukhopadhyay, R., Shaikh, A. M., Godwal, B. K., Eds.; Universities Press Limited: Telangana, India, 1998.
- (35) Barrio, M.; López, D. O.; Tamarit, J. L.; Negrier, P.; Haget, Y. *J. Mater. Chem.* **1995**, *5*, 431.
- (36) Fu, D.-W.; Zhang, W.; Cai, H.-L.; Zhang, Y.; Ge, J.-Z.; Xiong, R.-G.; Huang, S. D. *J. Am. Chem. Soc.* **2011**, *133*, 12780.